HHS Public Access

Author manuscript

Skeletal Radiol. Author manuscript; available in PMC 2017 March 01.

Published in final edited form as:

Skeletal Radiol. 2016 March ; 45(3): 383–391. doi:10.1007/s00256-015-2305-3.

High-Resolution Morphologic and Ultrashort Time-to-Echo Quantitative Magnetic Resonance Imaging of the Temporomandibular Joint

Won C Bae, PhD[2], **Monica Tafur, MD**[2], **Eric Y. Chang, MD**[1,2], **Jiang Du, PhD**[2], **Reni Biswas, BS**[2], **Kyu-Sung Kwack, MD PhD**[2], **Robert Healey, BS MBA**[2], **Sheronda Statum, MS MBA**[2], and **Christine B. Chung, MD**[1,2]

[1]Department of Radiology, Veterans Administration (VA) San Diego Healthcare System, 3350 La Jolla Village Drive, San Diego, CA 92161

[2]Department of Radiology, University of California, San Diego, School of Medicine, 408 Dickinson St., San Diego, CA 92103-8226

Abstract

Objective—To implement high-resolution morphologic and quantitative magnetic resonance imaging (MRI) of the temporomandibular joint (TMJ) using ultrashort time-to-echo (UTE) techniques in cadavers and volunteers.

Methods—This study was approved by the institutional review board. TMJs of cadavers and volunteers were imaged on a 3T-MR system. High-resolution morphologic and quantitative sequences using conventional and UTE techniques were performed in cadaveric TMJs. Morphologic and UTE quantitative sequences were performed in asymptomatic and symptomatic volunteers.

Results—Morphologic evaluation demonstrated the TMJ structures in open and closed-mouth position. UTE techniques facilitated the visualization of the disc and fibrocartilage. Quantitative UTE MRI was successfully performed ex-vivo and in-vivo reflecting the degree of degeneration. There was a difference in the mean UTE T2* values between asymptomatic and symptomatic volunteers.

Conclusions—MRI evaluation of the TMJ using UTE techniques allows characterization of the internal structure and quantification of the MR properties of the disc. Quantitative UTE MRI can be performed in-vivo with short scan times.

Introduction

Disorders of the temporomandibular joint (TMJ) are common and affect from 10% to 28% of the population [1,2]. Between 3–7% of the population seeks treatment for pain and

Corresponding author: Christine B. Chung, MD, 408 Dickinson Street, San Diego, CA 92103-8226, Office: (619) 471-0776, Fax: 619-471-0503, cbchung@ucsd.edu.

Conflict of Interest:

We have no conflicts of interest to disclose. All authors have read and approved the manuscript, the requirements for authorship have been met, and this manuscript represents honest work.

dysfunction of the TMJ or related structures [1]. The presence of symptoms such as clicks, limitation of oral aperture and pain, increase at more advance ages [2–4]. Damage to the TMJ disc has been shown to occur in the early stages of TMJ dysfunction before the appearance of any morphologic or positional changes [3,5].

Magnetic Resonance Imaging (MRI) has been accepted as the imaging modality of choice to assess TMJ disorders as it provides a non-invasive method of osseous and soft tissue visualization with excellent spatial and contrast resolution [4,6–8]. MR evaluation of the TMJ is useful to detect alterations in disc morphology or position, joint effusion and some of the signs related with osteoarthritis (OA) [2,7,8]. Furthermore, dynamic and pseudo-dynamic studies of the TMJ can be obtained with MRI as the patient opens and closes the mouth [9–11].

Despite the technological advances that have resulted in an improved visualization of the TMJ, conventional MRI techniques have some limitations. In the TMJ some tissues such as the cortical bone and the fibrocartilage present in the disc and in the articulating surfaces, have a majority of short T2 components [12–14]. As conventional MRI sequences use longer TEs, signal from those short T2 tissues has decayed before imaging acquisition [13–15].

Quantitative MRI techniques have been developed to map various MR imaging parameters, assessing the biochemical and structural changes that precede the morphologic findings observed in conventional MRI. These techniques have the ability to assess proteoglycan (PG) content, collagen content and orientation and water mobility in tissues, and are therefore sensitive to early degeneration. Quantitative techniques have been used mostly in the evaluation of articular cartilage and meniscus [16–25].

Recently implemented ultrashort time-to-echo (UTE) pulse sequences, which use much shorter TEs (down to 8 μs) as compared with conventional MRI, allow the detection of signal from tissues with short T2 components [13–15]. Quantitative MRI using UTE pulse sequences facilitate the evaluation of such tissues [26–30].

There are few articles published in the literature regarding quantitative MR evaluation of the TMJ. According with these studies, quantitative MRI (with UTE or conventional imaging) is a valid technique that facilitates characterization of the TMJ disc and may reflect the biomechanical and histochemical properties of the tissue [5,31].

In light of recent findings, it would be important to translate UTE quantitative techniques in vivo, to determine its sensitivity to diseases involving TMJ. The objectives of this study are: 1) to implement high-resolution morphologic and quantitative MRI of the TMJ using UTE techniques in cadaveric TMJs; and 2) to implement UTE quantitative MRI techniques in-vivo in symptomatic and asymptomatic volunteers.

Materials and Methods

The Institutional Review Board (IRB) exempted the cadaveric study and informed consent was not required. An IRB approval and informed consent were obtained for the volunteers MR imaging study.

Cadaveric Specimen Preparation

Skulls from four fresh cadavers were obtained (62–74 years, two females/two males) and two articular discs were dissected from two of the donors. The specimens were initially frozen at −40°C (Bio-Freezer; Forma Scientific, Marietta, OH) and thawed in saline for eight to twelve hours at room temperature prior to MR imaging.

Cadaveric Specimen MRI

Three cadaveric TMJs (from 2 donors) were imaged in a 3T Signa HDx scanner (GE Healthcare. Milwaukee, WI) using a modified transmit/receive switch and a 3-inch-surface coil placed adjacent to the TMJ. The two dissected articular discs (from two different donors) were imaged in the same MR system, using a custom-built transmit-receive solenoid.

High-resolution morphologic sequences were performed in the cadaveric TMJs and included: 1) sagittal fat saturated (FS) proton density (PD) fast spin echo (FSE) sequence (FOV = 8 cm, matrix = 384 × 384, slice thickness = 1.7 mm, TR = 2000 ms, TE = 30.10 ms, NEX = 2, scanning time = 8.6 mins); 2) sagittal non-fat saturated (NFS) PD FSE sequence (FOV = 8 cm, matrix = 384 × 384, slice thickness = 1.7 mm, TR = 2000 ms, TE = 40.4 ms, NEX = 2, scanning time = 8.6 mins); and 3) 2D UTE NFS sequence in the sagittal plane (FOV = 8 cm, matrix = 512 × 511, slice thickness = 1.7 mm, TR = 500 ms, TEs = 0.01 ms and 7.2 ms, NEX = 2, scanning time = 8.5 mins).

2D UTE pulse sequences employed a half radio frequency excitation pulse with radial mapping of k-space from center out followed by another half excitation with the polarity of the slice selection gradient reversed. Data from the 2 half excitations were added to produce a single radial line of k-space, repeated through 360 degrees, mapped onto a 512×512 grid and reconstructed by 2D inverse Fourier transformation [15,32,33].

High-resolution quantitative sequences were performed in the dissected articular discs and included: 1) UTE T2*; 2) UTE T1ρ; and 3) Spin Echo T2 sequences. T2* was measured through exponential fitting of UTE images with a series of TE delays [25,33]. The UTE T1ρ sequence combined a regular spin-lock pulse cluster followed by regular UTE acquisition. T1ρ was measured through exponential fitting of UTE T1ρ images acquired at a series of time-to-spin-lock (TSLs) [28,33]. T1 values required for calculating T1ρ were measured for each subject using saturation recovery UTE acquisitions with a series of saturation recovery time/projections. The parameters used in each sequence are detailed in Table 1.

In-Vivo MRI

TMJs of six volunteers (24 – 62 years; four females/two males; three asymptomatic and three symptomatic) were imaged in a 3T Signa HDx scanner (GE Healthcare. Milwaukee,

WI) using a modified transmit/receive switch and a 3-inch-surface coil place adjacent to the TMJ.

UTE T2* MR images employed similar UTE techniques to that of cadaveric quantitative analysis and were obtained in the sagittal plane. (Other quantitative sequences were not performed in vivo due to time consideration.) The parameters used in each sequence are detailed in Table 2. A sagittal T1 NFS FSE sequence was obtained for morphologic assessment of the TMJ (FOV = 10 cm, matrix = 512 × 512, slice thickness = 2.8 mm, TR = 700 ms, TE = 10.4 ms).

Morphologic Evaluation

Two subspecialized musculoskeletal radiologists (E.Y.C. and C.B.C. with 5 and 15 years of experience respectively) independently reviewed all the volunteers MR examinations using a Picture Archiving and Communication System workstation and were not aware of the presence or absence of symptoms. Images were evaluated for TMJ articular disc and mandibular condyle abnormalities. This morphologic assessment was done in the T1 NFS FSE sequence.

Disc morphology was catalogued as normal (biconcave) or abnormal (lengthened, biconvex, rounded, folded, thickened posterior band) and was evaluated for the presence of perforations [6,34–36]. The disc was also assessed for displacements within the joint in the sagittal plane and for changes in signal intensity [6,34–36]. Associated findings in the mandibular condyle were also evaluated and included subchondral plate morphology and bone marrow edema like signal [36–37].

Quantitative Evaluation

Regions of interest (ROIs) were drawn around each TMJ disc for each quantitative sequence, and both ROI values and pixel-by-pixel maps were determined based on signal intensity utilizing a nonlinear least square mono-exponential curve fitting program in MATLAB (MathWorks, R2011b). As described previously [28], UTE T1rho calculation takes into account T1 contamination due to incomplete recovery of the longitudinal magnetization from the use of relatively short TR values. The following equation was used to model T1rho relaxation in the presence of T1 contamination:

$$S(TSL) \propto \frac{e^{-TSL/T1rho}\left(1-e^{-(TR-TSL)/T1}\right)}{\left(1-e^{-TSL/T1rho}\right)\left(e^{-(TR-TSL)/T1}\right)cos\alpha} sin\alpha + C$$

S is the signal intensity, TSL is the spin lock time, TR is repetition time, T1 is longitudinal relaxation constant (measured from saturation recovery sequence), α is flip angle, and C is constant.

Similarly UTE T2* and spin echo T2 values were determined using the following equation modeling T2* or T2 relaxation:

$$S(TE) \propto 1 - e^{-TE/T2} + C$$

In addition to the fitted parameters, standard error of each fit was determined from the residual of the fit, where a smaller value indicates better fit.

Data Analysis

For cadaveric study, using EXCEL (V14.3.4, Microsoft) software, proportions of different morphologic findings in the articular disc and the mandibular condyle were determined. In addition, for quantitative MR measures, mean and standard deviation values were computed. However, due to small number of samples, statistical analysis was not performed.

For in-vivo study, the mean UTE T2* values between asymptomatic and symptomatic subjects were compared using analysis of variance.

Results

Cadaveric Study

The different structures of the TMJ were successfully demonstrated in the high-resolution PD MR images done in the cadaveric TMJs. In the sagittal PD FSE sequences, the articular disc was observed as a biconcave hypointense structure and its three portions were clearly visualized: anterior band, intermediate zone and posterior band. In the closed-mouth position the disc was located between the mandibular fossa of the temporal bone and the mandibular condyle (Figure 1). In the open-mouth position, the articular disc translated anteriorly and was located between the articular eminence of the temporal bone and the mandibular condyle. The superior and inferior retrodiscal layers, which form the retrodiscal tissue, separated from each other in the open-mouth position (Figure 2).

The 2D UTE pulse sequence with a TE of 0.01 ms, allowed the visualization of tissues with both long and short T2 components in the TMJ (Figure 3A). Subtraction techniques improved contrast between the articular disc and the surrounding structures. These techniques facilitate the visualization of structures with only short T2 components as MR images with longer TEs (Figure 3B) can be subtracted from MR images with shorter TEs. In the TMJ such short T2 structures are the fibrocartilaginous disc and the fibrocartilage covering of the articulating surfaces of the temporal bone and mandibular condyle (Figure 3C).

Internal structure of the articular disc was observed on high-resolution MR images of the dissected discs (Figures 4 and 5). The fibrocartilaginous matrix was best depicted at shorter TEs (0.1 – 2 ms) whereas the collagen network was best shown at longer TEs (10 – 11 ms) where the contrast between the two components was greater. The intermediate zone of one of the specimens had higher T2, UTE T2* and T1ρ values as compared with the anterior and posterior bands. In this specimen, the mean T2 value of the articular disc was 15.04 ms ± 0.97 ms, the mean UTE T2* value was 7.65 ms ± 0.15 ms and the mean T1ρ value was 9.62 ms ± 1.96 ms (Figure 4).

The second dissected disc was grossly abnormal and had a central perforation. In this specimen there was a prolongation in the T2, UTE T2* and UTE T1ρ relaxation times in the posterior band with a clear difference between the mean values of the posterior band (T2 = 58.02 ms ± 22.28 ms; UTE T2* = 14.26 ms ± 0.43 ms; UTE T1ρ = 17.46 ms ± 2.8 ms) as compared with the anterior band (T2 = 24.25 ms ± 5.78 ms; UTE T2* = 6.96 ms ± 0.2 ms; UTE T1ρ = 9.23 ms ± 1.37 ms) (Figure 5).

In-Vivo Quantitative Study

The age range of the total group of volunteers (n = 6) was 24–62 years (mean 38.17 years ± 16.19 years). The age range of the asymptomatic group of volunteers (n = 3) was 24–27 years (mean 24.33 years ± 2.52 years), two female and one male subject. The age range of the symptomatic group of volunteers (n = 3) was 47–62 years (mean 52 years ± 8.66 years), two female and one male subject. Symptoms included TMJ pain and clicking in one subject and TMJ pain in two subjects.

Morphologic analysis of the TMJ in the T1 NFS FSE sequence by the two radiologists, revealed signal intensity changes in all of the TMJ discs evaluated (n = 6). Five out of them (83.33%) had abnormalities in disc morphology. The only subject who had a normal morphology of the disc was symptomatic. Two discs were found to have anterior displacement (33.33%), one disc in an asymptomatic subject and one disc in a symptomatic subject. None were found to have posterior displacement. Additional MR findings in the mandibular condyle included thickening and irregularity of the subchondral plate in four of the six subjects (66.67%), two of them were asymptomatic and two were symptomatic. Bone marrow edema like signal and osteophytes at the anterior margin of the condyle were found in the symptomatic volunteer who referred TMJ pain and clicking (Figure 6).

The agreement between the two radiologists was perfect when diagnosing abnormal vs. normal articular discs. There was disagreement in one subject when characterizing the articular disc (described as perforated by one of the radiologist and described as abnormal without perforation by the other radiologist).

UTE T2* quantitative analysis was performed successfully in the six volunteers with short scanning times (average scan time of 3.2 minutes). UTE T2* mono-exponential fitting and color mapping analysis of the articular discs in the six subjects reflected the morphologic changes with prolongation in UTE T2* relaxation times at more advanced stages of degeneration (Figure 6). The range of mean UTE T2* values was 8.3 – 19.3 ms (mean 12.57 ms ± 3.86 ms). There was a slight increase (p=0.15) in the mean UTE T2* values of the disc in the symptomatic group (15.39 ms ± 3.43 ms) as compared with the asymptomatic group (9.74 ms ± 1.28 ms) (Figure 7).

Discussion

In this study UTE quantitative MRI was successfully performed in the TMJ of cadavers and subjects, allowing visualization of tissues with short T2 components and quantification of the MR properties of the articular disc. Mean T2, UTE T2* and UTE T1ρ values adequately reflected degenerative changes in cadaveric discs. Mean T1ρ values were overall higher than

mean UTE T2* values. Quantitative UTE MRI of the TMJ was performed in vivo using short scan times and was useful to assess the severity of articular disc degeneration. We found that the mean UTE T2* values of the articular disc in symptomatic volunteers showed a trend of being higher than in the asymptomatic group.

Integrity of the articular disc is essential for a normal function of the TMJ. Any alteration in the internal structure of the articular disc can affect its biomechanical properties and have a negative impact in the joint mechanics [38–41]. Damage to the TMJ disc has been shown to precede other morphologic or positional changes [3,5,41]. The ability to recognize early degenerative changes in the articular disc of the TMJ may be useful clinically if it precedes more serious structural deterioration in the TMJ, including disc perforation, rupture of the retrodiscal layers, joint space narrowing, changes in the articulating surfaces and the appearance of osteophytes [2,4,37].

With degeneration the tissue undergoes certain changes, which include an alteration in the collagen network, and a change in water and proteoglycan content [16,44–46]. The MR properties of the tissue will reflect the structural changes; therefore quantification of those properties is essential to recognize early alterations. As any fibrocartilaginous structure, the articular disc has short T2 components that cannot be evaluated with the standard MR techniques [13–15,31–33], that is why the application of UTE techniques is especially useful in the evaluation of the articular disc and other structures with short T2 components in the TMJ.

There is limited literature available regarding quantitative UTE MRI of the TMJ. Cao and Kakimoto performed T2 mapping of the articular disc demonstrating significant variations among the different portions of the disc [5] and prolongation of the T2 relaxation times of the disc with progressive degeneration [45]. Few studies have evaluated the application of UTE techniques in the TMJ [13,14,31]. Of these studies, the one by Sanal et al. quantified short T2* properties of the articular disc using UTE techniques with histologic and biomechanical reference standards in one cadaveric TMJ and in two asymptomatic volunteers. This study demonstrated an inverse relationship between UTE T2* values and indentation stiffness as well as collagen organization [31].

One of the limitations of this study was the small sample size. A second limitation was the availability of only T1 NFS FSE sequences for the morphological evaluation in the volunteers. The lack of fluid sensitive sequences may have affected the characterization of TMJ pathology by the radiologists. A third limitation was that signal intensity alterations in the discs, found in all volunteers, were attributed to pathology. Signal intensity alterations secondary to technical factors such as magic angle effects, motion artifacts and others were not considered.

In conclusion, MRI evaluation of the TMJ using UTE techniques allows characterization of the internal structure and quantification of the MR properties of the articular disc. Quantitative UTE MRI can be performed in-vivo with short scan times, to potentially monitor progressive changes in the TMJ disc associated with symptoms.

Acknowledgments

Funding received for this work:

VA Research and Rehabilitation Development – Chung

VA Clinical Research and Development – Chung

VA Clinical Science R&D Service – Chang

National Institute of Health – Chung, Bae, and Du

References

1. Poveda R, Bagán JV, Díaz JM, et al. Review of Temporomandibular Joint Pathology. Part I: classification, epidemiology and risk factors. Med Oral Patol Oral Cir Bucal. 2007; 12:E292–298. [PubMed: 17664915]
2. Tomas X, Pomes J, Berenguer J, et al. MR Imaging of Temporomandibular Joint Dysfunction: A Pictorial Review. Radiographics. 2006; 26:765–781. [PubMed: 16702453]
3. Tanaka E, Detamore MS, Mercuri LG. Degenerative Disorders of the Temporomandibular Joint: Etiology, Diagnosis, and Treatment. J Dent Res. 2008; 87:296–307. [PubMed: 18362309]
4. Aiken A, Bouloux G, Hudgins P. MR Imaging of the Temporomandibular Joint. Magn Reson Imaging Clin N Am. 2012; 20:397–412. [PubMed: 22877948]
5. Cao Y, Xia C, Wang S, et al. Application of magnetic resonance T2 mapping in the temporomandibular joints. Surg Oral Med Oral Pathol Oral Radiol. 2012; 114:644–649.
6. Orhan K, Nishiyama H, Tadashi S, et al. Comparison of altered signal intensity, position, and morphology of the TMJ disc in MR images corrected for variations in surface coil sensitivity. Oral Surg Oral Med Oral Pathol Oral Radiol Endod. 2006; 101:515–522. [PubMed: 16545717]
7. Foucart JM, Carpentier P, Pajoni D, et al. MR of 732 TMJs: anterior, rotational, partial and sideways disc displacements. Eur J Radiol. 1998; 28:86–94. [PubMed: 9717628]
8. Katzberg RW, Westesson PL, Tallents RH, et al. Temporomandibular Joint: MR Assessment of Rotational and Sideways Disk Displacements. Radiology. 1998; 169:741–748. [PubMed: 3186996]
9. Lin WC, Lo CP, Chiang IC, et al. The use of pseudo-dynamic magnetic resonance imaging for evaluating the relationship between temporomandibular joint anterior disc displacement and joint pain. Int J Oral Maxillofac Surg. 2012; 41:1501–1504. [PubMed: 22766070]
10. Wang EY, Mulholland TP, Pramanik BK, et al. Dynamic Sagittal Half-Fourier Acquired Single-Shot Turbo Spin-Echo MR Imaging of the Temporomandibular Joint: Initial Experience and Comparison with Sagittal Oblique Proton- Attenuation Images. AJNR Am J Neuroradiol. 2007; 28:1126–1132. [PubMed: 17569972]
11. Yen P, Katzberg RW, Buonocore MH, et al. Dynamic MR Imaging of the Temporomandibular Joint Using a Balanced Steady-State Free Precession Sequence at 3T. AJNR Am J Neuroradiol. 2013; 34:E24–26. [PubMed: 22033724]
12. Du J, Carl M, Bydder M, et al. Qualitative and quantitative ultrashort echo time (UTE) imaging of cortical bone. J Magn Reson. 2010; 207:304–311. [PubMed: 20980179]
13. Carl M, Sanal HT, Diaz E, et al. Optimizing MR Signal Contrast of the Temporomandibular Joint Disk. J Magn Reson Imaging. 2011; 34:1458–1464. [PubMed: 21972123]
14. Geiger D, Bae WC, Statum S, et al. Quantitative 3D ultrashort time-to-echo (UTE) MRI and micro-CT (μCT) evaluation of the temporomandibular joint (TMJ) condylar morphology. Skeletal Radiol. 2014; 43:19–25. [PubMed: 24092237]
15. Robson MD, Gatehouse PD, Bydder M, et al. Magnetic Resonance: An Introduction to Ultrashort TE (UTE) Imaging. J Comput Assist Tomogr. 2003; 27:825–846. [PubMed: 14600447]
16. Choi JA, Gold GE. MR Imaging of Articular Cartilage Physiology. Magn Reson Imaging Clin N Am. 2011; 19:249–282. [PubMed: 21665090]

17. Rauscher I, Stahl R, Cheng J, et al. Meniscal Measurements of T1ρ and T2 at MR Imaging in Healthy Subjects and Patients with Osteoarthritis. Radiology. 2008; 249:591–600. [PubMed: 18936315]
18. Li X, Ma CB, Link TM, et al. In vivo T1rho and T2 mapping of articular cartilage in osteoarthritis of the knee using 3 Tesla MRI. Osteoarthritis Cartilage. 2007; 15:789–797. [PubMed: 17307365]
19. Regatte RR, Akella SVS, Borthakur A, et al. In Vivo Proton MR Three-dimensional T1ρ Mapping of Human Articular Cartilage: Initial Experience. Radiology. 2003; 229:269–274. [PubMed: 14519880]
20. Hani AF, Kumar D, Malik AS, et al. Physiological assessment of in-vivo human knee articular cartilage using sodium MR imaging at 1.5 T. Magn Reson Imaging. 2013; 31:1059–1067. [PubMed: 23731535]
21. Madelin G, Babb J, Xia D, et al. Articular cartilage: evaluation with fluid-suppressed 7.0-T sodium MR imaging in subjects with and subjects without osteoarthritis. Radiology. 2013; 268:481–491. [PubMed: 23468572]
22. Williams A, Gillis A, McKenzie C, et al. Glycosaminoglycan distribution in cartilage as determined by delayed gadolinium-enhanced MRI of cartilage (dGEMRIC): potential clinical applications. AJR Am J Roentgenol. 2004; 182:167–172. [PubMed: 14684534]
23. Baum T, Joseph GB, Karampinos DC, et al. Cartilage and meniscal T2 relaxation time as non-invasive biomarker for knee osteoarthritis and cartilage repair procedures. Osteoarthritis Cartilage. 2013; 21:1474–1484. [PubMed: 23896316]
24. Mamisch TC, Trattnig S, Quirbach S, et al. Quantitative T2 Mapping of Knee Cartilage: Differentiation of Healthy Control Cartilage and Cartilage Repair Tissue in the Knee with Unloading - Initial Results. Radiology. 2010; 254:818–826. [PubMed: 20123898]
25. Andreisek G, Weiger M. T2* Mapping of Articular Cartilage: Current Status of Research and First Clinical Applications. Invest Radiol. 2014; 49:57–62. [PubMed: 24056113]
26. Williams A, Qian Y, Bear D, et al. Assessing degeneration of human articular cartilage with ultra-short echo time (UTE) T2* mapping. Osteoarthritis Cartilage. 2010; 18:539–546. [PubMed: 20170769]
27. Williams A, Qian Y, Golla S, et al. UTE-T2* mapping detects sub-clinical meniscus injury after anterior cruciate ligament tear. Osteoarthritis Cartilage. 2012; 20:486–494. [PubMed: 22306000]
28. Du J, Carl M, Diaz E, et al. Ultrashort TE T1rho (UTE T1rho) Imaging of the Achilles Tendon and Meniscus. Magn Reson Med. 2010; 64:834–842. [PubMed: 20535810]
29. Pauli C, Bae WC, Lee M, et al. Ultrashort–echo Time MR Imaging of the Patella with Bicomponent analysis: Correlation with Histopathologic and Polarized Light Microscopic Findings. Radiology. 2012; 264:484–493. [PubMed: 22653187]
30. Du J, Diaz E, Carl M, et al. Ultrashort Echo Time Imaging With Bicomponent Analysis. Magn Reson Med. 2012; 67:645–649. [PubMed: 22034242]
31. Sanal HT, Bae WC, Pauli C, et al. Magnetic Resonance Imaging of the Temporomandibular Joint Disc: Feasibility of Novel Quantitative Magnetic Resonance Evaluation Using Histologic and Biomechanical Reference Standards. J Orofac Pain. 2011; 25:345–353. [PubMed: 22247930]
32. Robson MD, Bydder GM. Clinical ultrashort echo time imaging of bone and other connective tissues. NMR Biomed. 2006; 19:765–780. [PubMed: 17075960]
33. Bae WC, Du J, Bydder GM, et al. Conventional and Ultrashort Time-to-Echo Magnetic Resonance Imaging of Articular Cartilage, Meniscus, and Intervertebral Disk. Top Magn Reson Imaging. 2010; 21:275–289. [PubMed: 22129641]
34. Incesu L, Taşkaya-Yilmaz N, Öğütcen-Toller M, et al. Relationship of condylar position to disc position and morphology. Eur J Radiol. 2004; 51:269–273. [PubMed: 15294336]
35. Taşkaya-Yilmaz N, Öğütcen-Toller M. Magnetic Resonance Imaging Evaluation of Temporomandibular Joint Disc Deformities in Relation to Type of Disc Displacement. Oral Maxillofac Surg. 2001; 59:860–865.
36. Milano V, Desiate A, Bellino R, et al. Magnetic resonance imaging of temporomandibular disorders: classification, prevalence and interpretation of disc displacement and deformation. Dentomaxillofac Radiol. 2000; 29:352–361. [PubMed: 11114665]

37. Honda K, Natsumi Y, Urade M. Correlation between MRI evidence of degenerative condylar surface changes, induction of articular disc displacement and pathological joint sounds in the temporomandibular joint. Gerodontology. 2008; 25:251–257. [PubMed: 18312371]
38. Gross A, Bumann A, Hoffmeister B. Elastic fibers in the human temporomandibular joint disc. Int J Oral Maxillofac Surg. 1999; 28:464–468. [PubMed: 10609752]
39. Sindelar BJ, Herring SW. Soft Tissue Mechanics of the Temporomandibular Joint. Cells Tissues Organs. 2005; 180:36–43. [PubMed: 16088132]
40. Tanaka E, van Eljden T. Biomechanical Behavior of the Temporomandibular Joint Disc. Crit Rev Oral Biol Med. 2003; 14:138–150. [PubMed: 12764076]
41. Sharawy M, Ali AM, Choi WS, et al. Ultrastructural Characterization of the Rabbit Mandibular Condyle following Experimental Induction of Anterior Disk Displacement. Cells Tissues Organs. 2000; 167:38–48. [PubMed: 10899715]
42. Borthakur A, Mellon E, Niyogi S, et al. Sodium and T1 rho MRI for molecular and diagnostic imaging of articular cartilage. NMR Biomed. 2006; 19:781–821. [PubMed: 17075961]
43. Blumenkrantz G, Majumdar S. Quantitative magnetic resonance imaging of articular cartilage in osteoarthritis. Eur Cell Mater. 2007; 13:75–86.
44. Dijkgraaf LC, deBont LG, Boering G, et al. The structure, biochemistry, and metabolism of osteoarthritis cartilage: a review of the literature. J Oral Maxillofac Surg. 1995; 53:1182–1192. [PubMed: 7562173]
45. Kakimoto N, Shimamoto H, Chindasombatjaroen J, et al. Comparison of the T2 Relaxation Time of the Temporomandibular Joint Articular Disk between Patients with Temporomandibular Disorders and Asymptomatic Volunteers. AJNR Am J Neuroradiol. 2014 Apr 17. [Epub ahead of print].

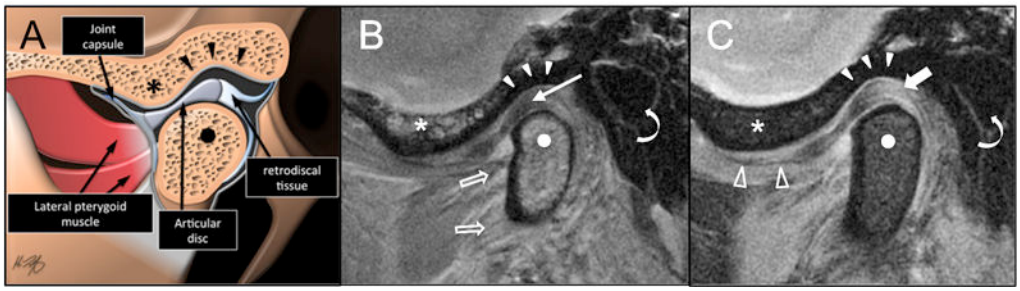

Figure 1.

Illustration (A), high-resolution PD FSE NFS (B) and FS (C) MR images of the Temporomandibular Joint (TMJ) in the closed-mouth position in the sagittal plane. When the mandible is closed, the posterior band of the articular disc (arrow) lies between the mandibular condyle (points) and the mandibular fossa of the temporal bone (arrowheads). Retrodiscal tissue or bilaminar zone = thick arrow; articular eminence of the temporal bone = *; lateral pterygoid muscle = open arrows; superior attachment of the joint capsule = open arrowheads; external auditory canal = curved arrows.

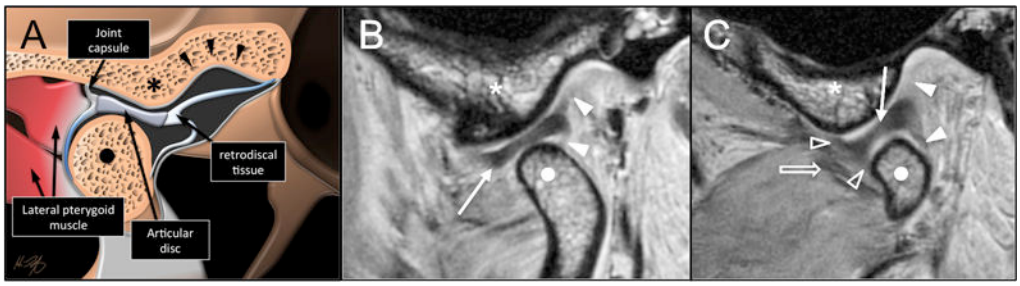

Figure 2.

Illustration (A) and high-resolution PD FSE NFS sagittal MR images in the open-mouth position at the center (B) and medial aspect (C) of the mandibular condyle (points). As the mouth opens the articular disc (white arrow) translates anteriorly and locates between the articular eminence (●) and the condyle. The superior and inferior retrodiscal layers (white arrowheads) separate as the mouth opens. Capsular attachments = open arrowheads; lateral pterygoid muscle (open arrow).

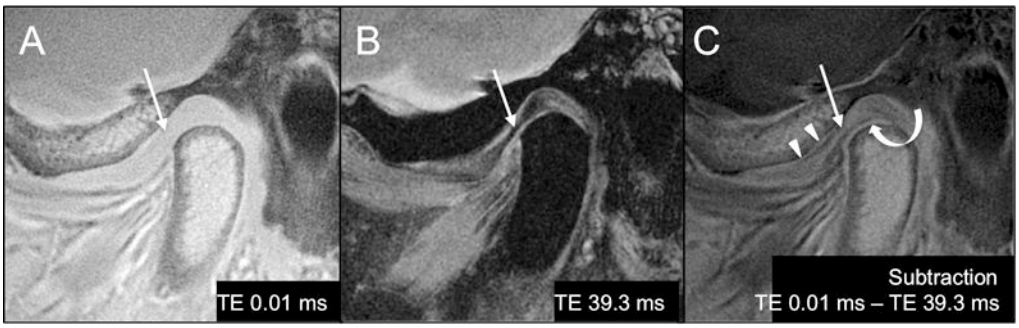

Figure 3.

A. 2D UTE NFS (TR 500 ms/TE 0.01 ms), B. PD FS FSE (TR 2000 ms/TE 39.3 ms) and C. subtraction MR images (TE 0.01 ms – TE 39.3 ms) of the TMJ in the sagittal plane. The fibrocartilaginous articular disc (arrows) has mean short T2 values and it is hyperintense with short TEs (arrow in A). With longer TEs, its signal decays rapidly and the disc looks hypointense (arrow in B). Subtraction (C) of the PD MR image (B), which only demonstrate tissues with long T2 values from the UTE MR image (A), which demonstrates tissues with both short and long T2 components, facilitate the identification of the structures with only short T2 components such as the articular disc (arrow in C) and the fibrocartilaginous cover of the articulating surfaces of the condyle (curved arrow) and mandibular fossa (arrowheads).

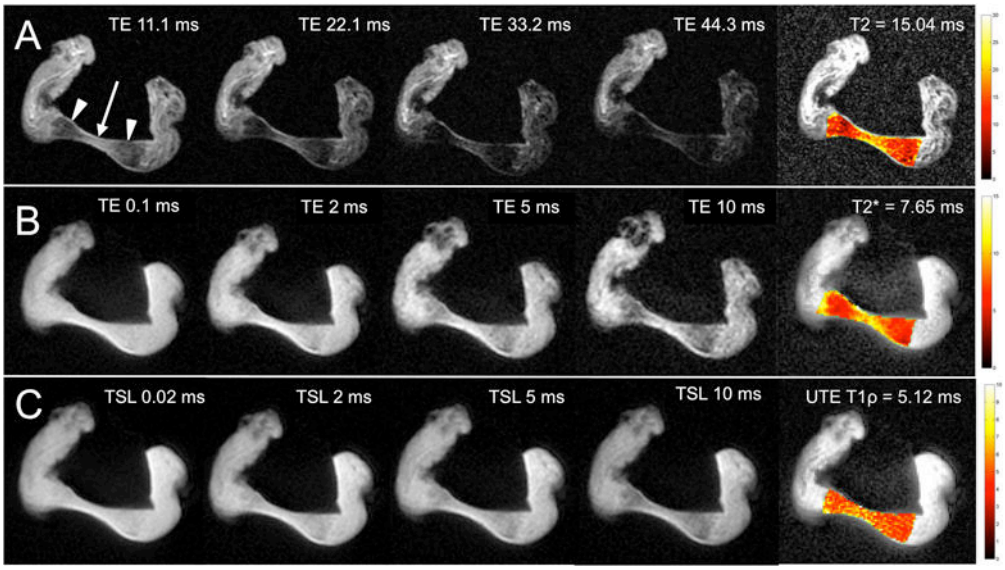

Figure 4.

A. Sagittal T2 SE MR images and color mapping of a cadaveric TMJ articular disc at a series of TEs (11.1, 22.1, 33.2 and 44.3 ms). B. Sagittal UTE T2* MR images and color mapping of the same articular disc at a series of TEs (0.1, 2, 5 and 10 ms). C. Sagittal UTE T1ρ MR images and color mapping of the same articular disc at a series of spin-lock times (TSL) (0.02, 2, 5 and 10 ms). At the anterior and posterior bands of the disc (arrowheads), the signal decays fast with increasing TEs. In contrast, the intermediate zone (arrow) has higher signal intensity with longer TEs. UTE T1ρ MR images show less signal loss with increasing TSLs as compared with the UTE T2* with increasing TEs. T2, UTE T2* and UTE T1ρ values are lower at the anterior and posterior bands of the disc as compared with the intermediate zone. This is reflected in the color maps.

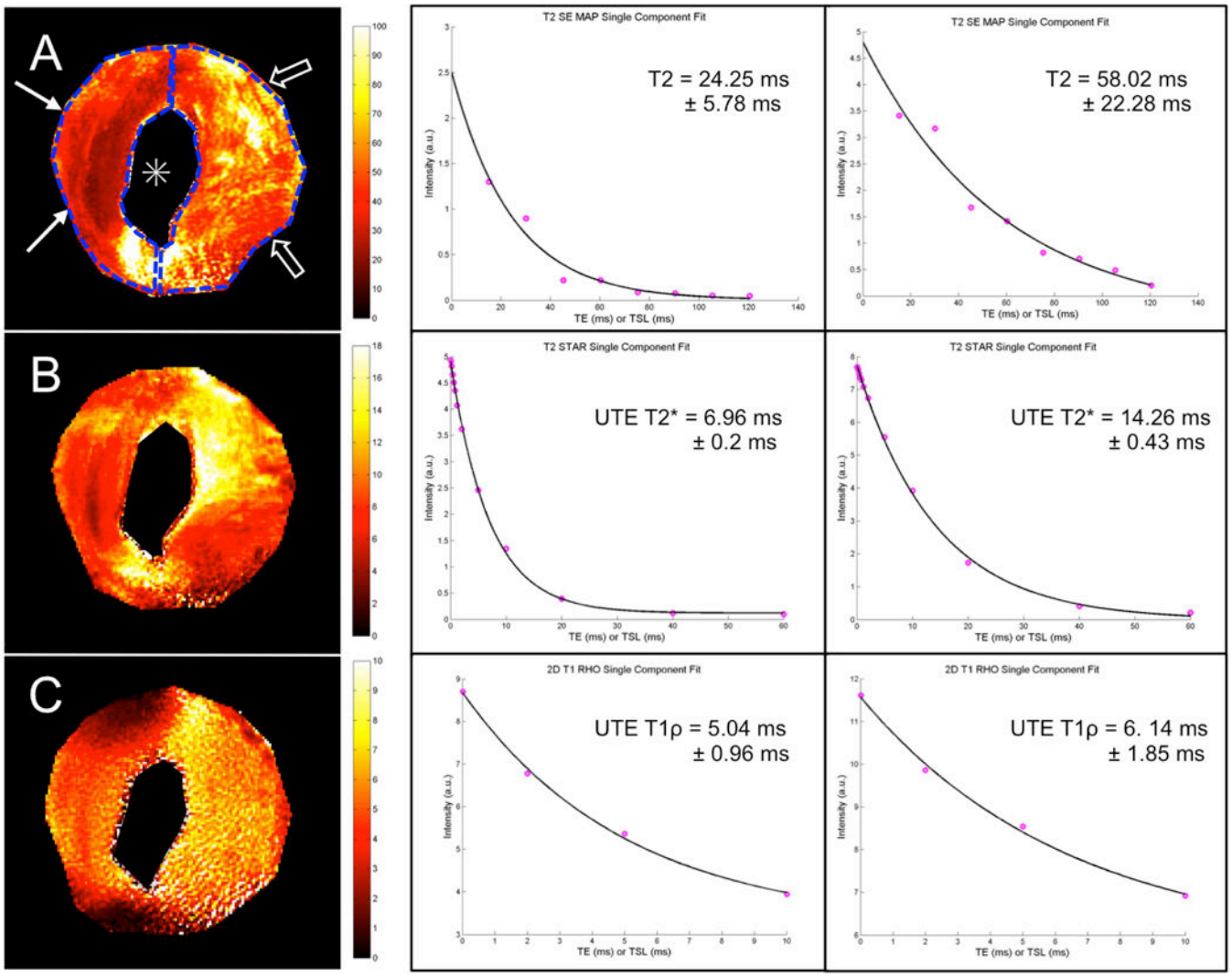

Figure 5.

T2 SE (A), UTE T2* (B), and UTE T1ρ (C) color mapping in the axial plane (left) and mono-exponential fitting (center and right) of an abnormal cadaveric TMJ articular disc with a central perforation (*). When analyzing two different ROIs located at the anterior and posterior bands respectively, an increase in the mean T2, UTE T2* and UTE T1ρ values in the posterior band of the disc (open arrows) (58.02 ms, 14.26 ms and 6.14 ms respectively) as compared with the anterior band (arrows) (24.25 ms, 6.96 ms and 5.04 ms respectively) was demonstrated. This finding could be secondary to tissue degeneration adjacent to the central perforation (*****).Fitted value ± standard error are shown on the plots.

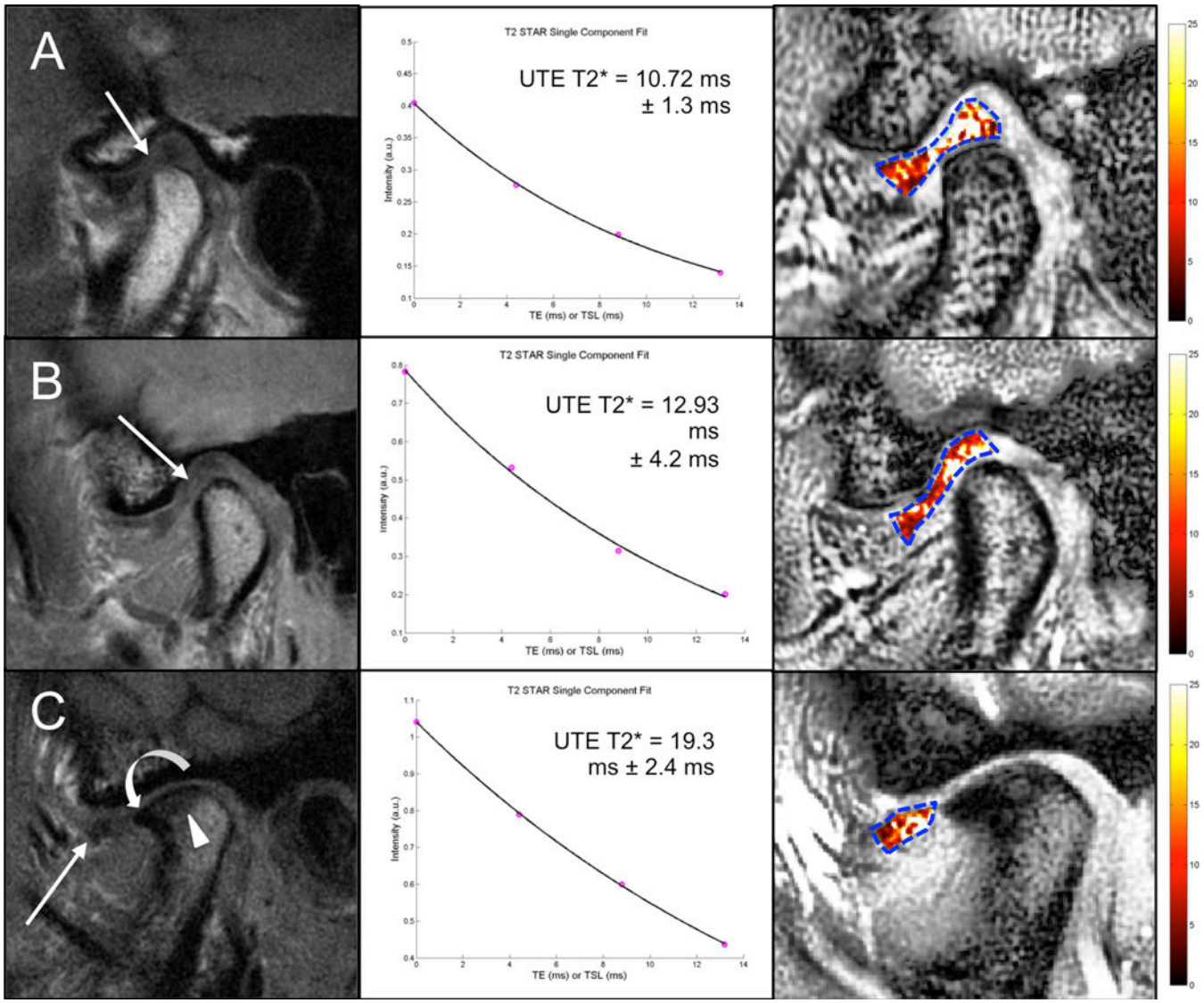

Figure 6.

Sagittal T1 NFS FSE MR images (left), UTE T2* mono-exponential fitting (center) and color mapping (right) of the articular disc of the TMJ in an asymptomatic subject (A), in a symptomatic subject with TMJ pain (B), and in a symptomatic subject who complained of pain and clicking in the right TMJ (C). A. The disc has a biconcave morphology with a focal area of hyperintensity in the intermediate zone and the anterior portion of the posterior band (arrow). B. The disc has a lengthened morphology with diffuse signal heterogeneity especially in the intermediate zone and the posterior band (arrow). C. There is anterior displacement of the articular disc, which appears small and irregular in shape with diffuse altered signal intensity especially to its posterior aspect (arrow). Associated findings in the mandibular condyle include thickening and irregularity of the subchondral bone plate and an osteophyte formation in the anterior margin of the condyle. In all subjects (A, B and C), color maps reflect the morphologic findings with increasing UTE T2* values at more advanced stages of disc alteration.

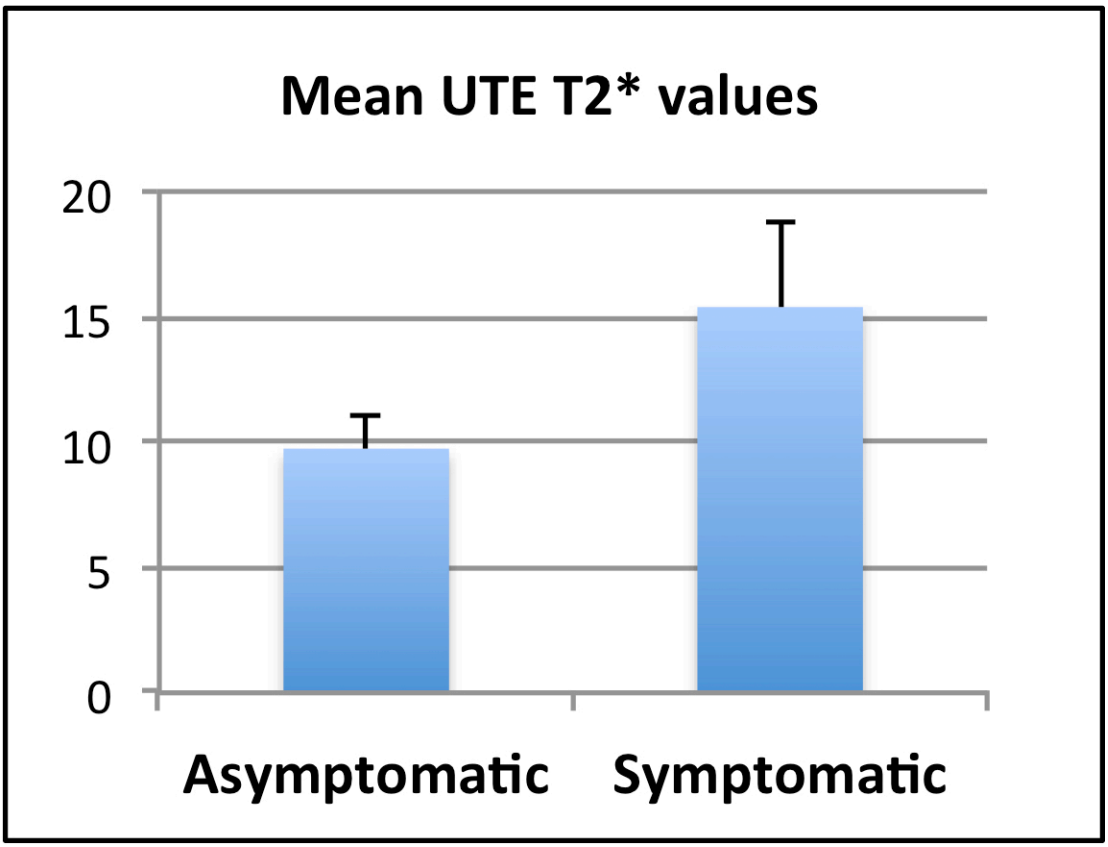

Figure 7.
Graph showing the mean UTE T2* values in the asymptomatic and symptomatic groups. Mean UTE T2* values tended to be higher in the symptomatic group.

Table 1

Protocol used for Cadaveric Quantitative MR Imaging

Parameters	T2 SE	UTE T2*	UTE T1ρ	UTE T1 TSR
Repetition Time (ms)	2000	100	300	28, 43,68,118, 218,418,818,1618
Echo Time (ms)	11,22,33,44,55,66,77,88	0.1, 0.2, 0.4, 0.6, 0.8,1.2,2,5,10,20,40,60	0.008	0.008
Spin-Lock Time (ms)	N/A	N/A	0.02, 2,5,10	N/A
Field of View (cm)	10	10	10	10
Matrix	320 × 256	512 × 512	256 × 255	320 × 299
Slice Thickness (mm)	1.5	3	3	3
NEX	1	2	2	1
Flip Angle	90	40	40	40
Scan Time (min)	10.9	12.7	27.1	19.1

MR = Magnetic Resonance; SE = Spin Echo; UTE = Ultrashort Time-to-Echo; TSR = Saturation Recovery Time; NEX = Number of excitations.

Table 2

Protocol used for In-Vivo Quantitative MR Imaging

Parameters	UTE T2*
Repetition Time (ms)	300
Echo Time (ms)	0.01, 4.4, 8.8, 13.2
Spin-Lock Time (ms)	N/A
Field of View (cm)	10
Matrix	512 × 512
Slice Thickness (mm)	2.8
NEX	2
Flip Angle	45
Scan Time (min)	3.2

MR = Magnetic Resonance; UTE = Ultrashort Time-to-Echo; NEX = Number of excitations.